

Antennas and Reaction Centers of Photosynthetic Bacteria

Structure, Interactions, and Dynamics

Proceedings of an International Workshop
Feldafing, Bavaria, F.R.G., March 23–25, 1985

Editor: M. E. Michel-Beyerle

With 168 Figures

Springer-Verlag
Berlin Heidelberg New York Tokyo

Contents

Part I Antennas: Structure and Energy Transfer

Structure of Antenna Polypeptides. By H. Zuber	2
The Crystal and Molecular Structure of C-Phycocyanin By R. Huber	15
C-Phycocyanin from <i>Mastigocladus laminosus</i> . Isolation and Properties of Subunits and Small Aggregates. By W. John, R. Fischer, S. Siebzehnrübl, and H. Scheer (With 9 Figures)	17
Picosecond Time-Resolved, Polarized Fluorescence Decay of Phycobilisomes and Constituent Biliproteins Isolated from <i>Mastigocladus laminosus</i> By S. Schneider, P. Geiselhart, T. Mindl, F. Dörr, W. John, R. Fischer, and H. Scheer (With 4 Figures)	26
Fluorescence Behaviour of Crystallized C-Phycocyanin (Trimer) from <i>Mastigocladus laminosus</i> By S. Schneider, P. Geiselhart, C. Scharnagl, T. Schirmer, W. Bode, W. Sidler, and H. Zuber (With 4 Figures)	36
Energy-Transfer Kinetics in Phycobilisomes By A.R. Holzwarth (With 2 Figures)	45
Exciton State and Energy Transfer in Bacterial Membranes: The Role of Pigment-Protein Cyclic Unit Structures By R.M. Pearlstein and H. Zuber	53
Carotenoid-Bacteriochlorophyll Interactions By R.J. Cogdell (With 1 Figure)	62
Bacteriochlorophyll <i>a</i> - and <i>c</i> -Protein Complexes from Chlorosomes of Green Sulfur Bacteria Compared with Bacteriochlorophyll <i>c</i> Aggregates in CH_2Cl_2 -Hexane. By J.M. Olson, P.D. Gerola, G.H. van Brakel, R.F. Meiburg, and H. Vasmel (With 8 Figures) ...	67
Reverse-Phase High-Performance Liquid Chromatography of Antenna Pigment- and Chlorosomal Proteins of <i>Chloroflexus</i> <i>aurantiacus</i> . By R. Feick (With 2 Figures)	74

Fluorescence-Detected Magnetic Resonance of the Antenna Bacteriochlorophyll Triplet States of Purple Photosynthetic Bacteria. By A. Angerhofer, J.U. von Schütz, and H.C. Wolf (With 1 Figure)	78
High-Resolution ^1H NMR of Light-Harvesting Chlorophyll-Proteins. By C. Dijkema, G.F.W. Searle, and T.J. Schaafsma	81
Crystallization and Linear Dichroism Measurements of the B800-850 Antenna Pigment-Protein Complex from <i>Rhodopseudomonas sphaeroides</i> 2.4.1 By J.P. Allen, R. Theiler, and G. Feher (With 2 Figures)	82
Crystallization of the B800-850-complex from <i>Rhodopseudomonas acidophila</i> Strain 7750 By R.J. Cogdell, K. Woolley, R.C. Mackenzie, J.G. Lindsay, H. Michel, J. Dobler, and W. Zinth (With 6 Figures)	85
Linear Dichroism (LD) and Absorption Spectra of Crystals of B800-850 Light-Harvesting Complexes of <i>Rhodopseudomonas capsulata</i> . By W. Mantele, K. Steck, T. Wacker, W. Welte, B. Levoir, and J. Breton (With 5 Figures)	88

Part II Reaction Centers: Structure and Interactions

The Crystal Structure of the Photosynthetic Reaction Center from <i>Rhodopseudomonas viridis</i> By J. Deisenhofer and H. Michel (With 2 Figures)	94
Single Crystals from Reaction Centers of <i>Rhodopseudomonas viridis</i> Studied by Polarized Light. By W. Zinth, M. Sander, J. Dobler, W. Kaiser, and H. Michel (With 3 Figures)	97
On the Analysis of Optical Spectra of <i>Rhodopseudomonas viridis</i> Reaction Centers By E.W. Knapp and S.F. Fischer (With 3 Figures)	103
Orientation of the Chromophores in the Reaction Center of <i>Rhodopseudomonas viridis</i> . Comparison of Low-Temperature Linear Dichroism Spectra with a Model Derived from X-Ray Crystallography. By J. Breton (With 4 Figures)	109
Calculations of Spectroscopic Properties of Bacterial Reaction Centers. By W.W. Parson, A. Scherz, and A. Warshel (With 5 Figures)	122
On the Temperature-Dependence of the Long Wavelength Fluorescence and Absorption of <i>Rhodopseudomonas viridis</i> Reaction Centers. By P.O.J. Scherer, S.F. Fischer, J.K.H. Hörber, M.E. Michel-Beyerle, and H. Michel (With 3 Figures)	131

Local Environments of Pigments in Reaction Centers of Photosynthetic Bacteria from Resonance Raman Data By M. Lutz and B. Robert (With 4 Figures)	138
The Spin-Polarization Pattern of the $\Delta m = 1$ Triplet EPR Spectrum of <i>Rps. viridis</i> Reaction Centers By F.G.H. van Wijk, P. Gast, and T.J. Schaafsma	146
Triplet State Investigation of Charge Separation and Symmetry in Single Crystals of <i>R. viridis</i> Reaction Centers By J.R. Norris, D.E. Budil, H.L. Crespi, M.K. Bowman, P. Gast, C.P. Lin, C.H. Chang, and M. Schiffer	147
Triplet-minus-Singlet Absorbance Difference Spectroscopy of Photosynthetic Reaction Centers by Absorbance-Detected Magnetic Resonance. By A.J. Hoff (With 11 Figures)	150
ENDOR Studies of the Primary Donor in Bacterial Reaction Centers. By W. Lubitz, F. Lendzian, M. Plato, K. Möbius, and E. Tränkle (With 6 Figures)	164
ENDOR of Semiquinones in RCs from <i>Rhodopseudomonas sphaeroides</i> . By G. Feher, R.A. Isaacson, M.Y. Okamura, and W. Lubitz (With 10 Figures)	174
Photoinduced Charge Separation in Bacterial Reaction Centers Investigated by Triplets and Radical Pairs By J.R. Norris, D.E. Budil, S.V. Kolaczkowski, J.H. Tang, and M.K. Bowman (With 5 Figures)	190
Spin Dipolar Interactions of Radical Pairs in Photosynthetic Reaction Centers. By A. Ogrodnik, W. Lersch, M.E. Michel-Beyerle, J. Deisenhofer, and H. Michel (With 4 Figures)	198
Protein/Lipid Interaction of Reaction Center and Antenna Proteins. By J. Riegler, W.M. Heckl, J. Peschke, M. Lösche, and H. Möhwald (With 6 Figures)	207
The Architecture of Photosystem II in Plant Photosynthesis. Which Peptide Subunits Carry the Reaction Center of PS II? By A. Trebst and B. Depka (With 3 Figures)	216

Part III Electron-Transfer: Theory and Model Systems

Application of Electron-Transfer Theory to Several Systems of Biological Interest. By R.A. Marcus and N. Sutin	226
Effects of Distance, Energy and Molecular Structure on Long-Distance Electron-Transfer Between Molecules By J.R. Miller (With 4 Figures)	234

Ultrafast Electron Transfer in Biomimetic Models of Photosynthetic Reaction Centers. By M.R. Wasielewski, M.P. Niemczyk, W.A. Svec, and E.B. Pewitt (With 5 Figures)	242
Electron Transfer Through Aromatic Spacers in Bridged Electron-Donor-Acceptor Molecules. By H. Heitele and M.E. Michel-Beyerle	250
Electron Transfer in Rigidly Linked Donor-Acceptor Systems By S.F. Fischer, I. Nussbaum, and P.O.J. Scherer (With 3 Figures)	256
Electron Conduction Along Aliphatic Chains By R. Bittl, H. Treutlein, and K. Schulten (With 4 Figures)	264

Part IV Reaction Centers: Structure and Dynamics

Kinetics and Mechanisms of Initial Electron-Transfer Reactions in <i>Rhodopseudomonas sphaeroides</i> Reaction Centers By W.W. Parson, N.W.T. Woodbury, M. Becker, C. Kirmaier, and D. Holten (With 3 Figures)	278
Femtosecond Studies of the Reaction Center of <i>Rhodopseudomonas viridis</i> : The Very First Dynamics of the Electron-Transfer Processes. By W. Zinth, M.C. Nuss, M.A. Franz, W. Kaiser, and H. Michel (With 5 Figures)	286
Analysis of Time-resolved Fluorescence of <i>Rhodopseudomonas viridis</i> Reaction Centers By J.K.H. Hörber, W. Göbel, A. Oggodnik, M.E. Michel-Beyerle, and E.W. Knapp (With 3 Figures)	292
The Characterization of the Q _A Binding Site of the Reaction Center of <i>Rhodopseudomonas sphaeroides</i> . By M.R. Gunner, B.S. Braun, J.M. Bruce, and P.L. Dutton (With 2 Figures)	298

Part V Model Systems on Structure of Antennas and Reaction Centers

Structure and Energetics in Reaction Centers and Semi-synthetic Chlorophyll Protein Complexes. By S.G. Boxer (With 4 Figures) ..	306
Small Oligomers of Bacteriochlorophylls as <i>in vitro</i> Models for the Primary Electron Donors and Light-Harvesting Pigments in Purple Photosynthetic Bacteria By A. Scherz, V. Rosenbach, and S. Malkin (With 7 Figures)	314
Experimental, Structural and Theoretical Models of Bacteriochlorophylls a, d and g. By J. Fajer, K.M. Barkigia, E. Fujita, D.A. Goff, L.K. Hanson, J.D. Head, T. Horning, K.M. Smith, and M.C. Zerner (With 6 Figures)	324

ENDOR Characterization of Hydrogen-Bonding to Immobilized Quinone Anion Radicals. By P.J. O'Malley, T.K. Chandrashekhar, and G.T. Babcock (With 3 Figures)	339
Concluding Remarks. Some Aspects of Energy Transfer in Antennas and Electron Transfer in Reaction Centers of Photosynthetic Bacteria. By J. Jortner and M.E. Michel-Beyerle (With 6 Figures)	345
Index of Contributors	367

C-Phycocyanin from *Mastigocladus laminosus*. Isolation and Properties of Subunits and Small Aggregates

W. John, R. Fischer, S. Siebzehnrübl, and H. Scheer

Institut für Botanik der Universität München, Menzinger Str. 67
D-8000 München 19, F. R. G.

1. Introduction

Photosynthetic organisms cover most of their energy needs with sunlight. They have consequently developed a variety of adaptation mechanisms to compete efficiently for it. In higher plants, a dominant mechanism is the growth towards the light. Aquatic and microorganisms adapt commonly by chromatic adaptation of the photosynthetic antenna. The chlorophylls a and b are rather inefficient in collecting green light, and several additional pigment systems have evolved to fill this hole in the action spectrum.

The phycobiliproteins comprise one such group of antenna pigments. They are used in cyanobacteria, red alga and cryptophytes (1). In the former two, they are highly aggregated together with colorless linker polypeptides (2), in the phycobilisomes (3). These are microscopic structures situated at the outer surface of the thylakoid membrane, which transfer their excitation energy efficiently (quantum yield 295%) to the chlorophyllous reaction centers within the membrane. In cooperation with the group of S. SCHNEIDER (Garching), we have recently begun to study the fluorescence properties of small aggregates and subunits of phycocyanins (4). The aim of this work is an understanding of the energy transfer in these pigments in relation to the size and structure of the assembly. This report is concerned with the stability and the photochemical reactivity of C- phycocyanin (PC) and its subunits from *M. laminosus*. Time- resolved polarized fluorescence data are presented in the accompanying report of the Garching group.

2. Materials and Methods

M. laminosus was grown in suspension culture in CASTENHOLZ medium (5). C- PC was isolated as reported earlier (4). The subunits were isolated by preparative electrofocusing on Agarose gels (Pharmacia, München) in 8M urea, and renatured without delay on a desalting column (Biogel P6, Biorad).

Absorption spectra were recorded on a model 320 (Perkin Elmer, Überlingen) spectrophotometer. The cell holder was thermostated, and temperatures measured in the cuvettes with a Pt 100 resistor. Absorption difference spectra were measured with a ZWS II dual- wavelength photometer (Sigma, Berlin) in split- beam mode. The data were digitized and stored with model II+ computer (Apple, München) using a self- made program, which was developed for obtaining high wavelength accuracy.

Fluorescence spectra were recorded on a DMR 22 (Zeiss, Oberkochen) spectrofluorimeter. The cell holders were thermostated, and the

temperatures recorded in the cuvettes with a Pt 100 resistor. The spectra are uncorrected for the spectral response function of the apparatus. Circular dichroism spectra were recorded on a model Mark V dichrograph (Jobin- Yvon ISA, München) equipped with a silex computer (Leanord, Lille) and a modified software. Sedimentation coefficients were obtained in a model E ultracentrifuge (Beckman, München) at 20°C with the scanner wavelength set at 620nm.

Chemicals and solvents were reagent grade unless otherwise stated. Sodium dodecyl sulfate- polyacrylamide electrophoresis was done by the method of LAEMMLI (6).

3. Results

3.1 Optical Spectra

All studies were done in potassium phosphate buffer (50 or 100mM) at pH7.5. Under these conditions, PC is isolated as a trimer (heterohexamer, $(\alpha\beta)$, sedimentation coefficient $\approx 4.8S$). It can be dissociated reversibly into the monomer (heterodimer, $(\alpha\beta)_2$, $\approx 2.8S$) by incubation with potassium thiocyanate. The absorption spectrum of the monomer is slightly blue- shifted as compared to the trimer, but otherwise very similar (fig. 1).

The spectra shown in fig. 1 correspond to preparations, which are free of colorless linker- peptides. If the latter are present, the spectra of monomers (obtained by the same dissociation method) remain unchanged. The trimer spectra are more strongly red- shifted, however, and a series of slightly different species absorbing between 620 and 638nm can be isolated. Their sedimentation coefficients are only slightly higher ($\approx 6S$) than that of the trimer. This is due to the presence of varying amounts of several colorless linker- peptides. The exact stoichiometry is still under investigation. An increased chromophore- chromophore coupling in these red- shifted complexes is suggested from their circular dichroism (CD) spectra. Simultaneously with the red- shift in the absorption maximum, there develops a pronounced red- shifted feature in the CD- spectrum, which increases with an increasing red- shift (fig. 2). It has been rationalized as an S- shaped exciton couplet (positive at longer wavelengths), which is superimposed on the absorption- type CD- spectrum of the monomer.

Exciton couplings are absent in linker-peptide-free preparations of PC from M. laminosus, but have been discussed earlier in PC from S. platensis (7) and in particular in allophycocyanins (8). The induction of exciton coupling would require a changed geometry of the chromophores, which can be considered on the basis of the x-ray structure of trimeric PC from the same organism (9; see also SCHIRMER et al., this monograph). The closest chromophore contacts in the linker-peptide-free trimer are between the α - chromophore of the monomeric unit and the β_1 - chromophore of the adjacent one. The center- to- center distance (22A) is just too large for exciton interactions. Changes by only a few Angström may, however, be sufficient to allow for strong couplings, and it is possible that such changes are induced by the linker-peptides. Unless there is a gross structural change involved, the red- shifted species are then most likely due to a changed geometry in the contact region of the monomeric units.

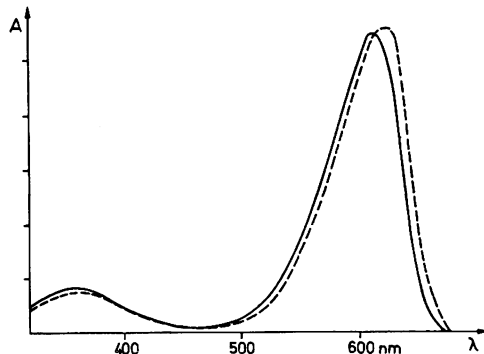


Fig. 1: Absorption spectra of monomeric ($\alpha\beta$, —) and trimeric ($(\alpha\beta)_3$; ---) PC from M. laminosus (50mM phosphate buffer, pH 7.5)

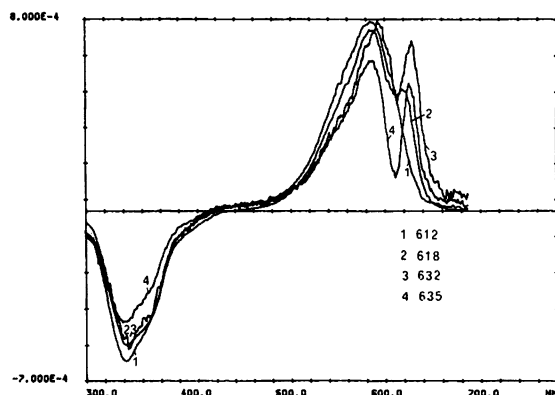


Fig. 2: Circular dichroism spectra of trimeric phycocyanin containing linker peptides: aggregates with increasing wavelength of the red absorption band. λ_{max} see inserts.

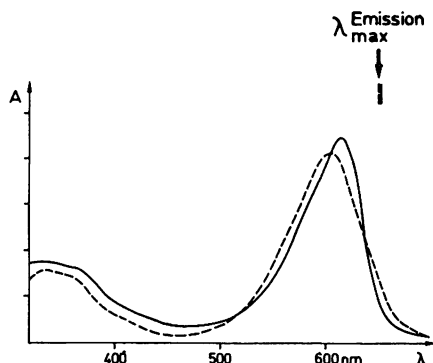


Fig. 3: Absorption spectra of the isolated subunits of PC from M. laminosus (α : —; β : ---). The emission maxima are indicated by the labels in the upper right.

The absorption spectra of the isolated subunits (fig.3) show considerable differences both with respect to the position and the shape of the long-wavelength band. The α -subunit ($\lambda_{\text{max}} = 616\text{nm}$) has a narrow band similar in shape to that of integral PC, whereas the β -subunit has a blue-shifted ($\lambda_{\text{max}} = 605\text{nm}$) and broadened band. The weighed sum of the two absorption spectra is very similar to that of monomeric PC (not shown). In spite of this blue-shifted absorption, the fluorescence maxima are almost at the same position (fig.3). The α -subunit carries one chromophore, the β -subunit two chromophores (β_1, β_2) at different binding sites of the apoprotein (10), the broadening should then reflect a slight difference in the excitation energies of the two chromophores. This is indeed supported by the circular dichroism spectra (fig.4). The anisotropy of the β -subunit is only $\approx 60\%$ as compared to the α -subunit. The positive extremum is considerably blue-shifted with respect to the absorption maximum, and there is a low-intensity red-wing in the CD-spectrum. It is suggested that the β -subunit carries one optically active (planar?) chromophore ($\lambda_{\text{max}} \approx 595\text{nm}$) and one much less active (planar?) chromophore ($\lambda_{\text{max}} \approx 615\text{nm}$).

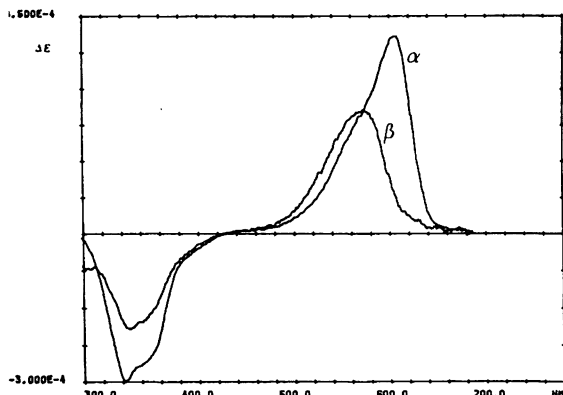


Fig. 4: CD of the isolated subunits shown in Fig. 2 (α : —; β : - - -). The spectra are normalized to equal absorptions in the long-wavelength maximum.

This interpretation is supported by similar CD data and additional fluorescence polarisation results of MIMURO et al. (this volume). An assignment of the individual chromophores on the β -subunit to the such defined absorptions is not yet possible. Based on the amino-acid sequence and the x-ray structure (9,10), β_1 is similar to α . The absorption maxima would then relate β_1 to the chromophore absorbing at $\approx 615\text{nm}$. Since these chromophores come closest in the trimer, the exciton split at the red wing of the main CD-band in linker-associated trimers (vide supra) would support this assignment. However, the CD-data suggest a rather different conformation for the β -chromophore ($\lambda_{\text{max}} \approx 615\text{nm}$) and the α -chromophore, and biochemical labeling will be necessary to decide this point conclusively.

3.2 Stabilities

The chromophores of PC are held rigidly in an energetically unfavorable, extended conformation (1,9). This conformation is due to non-covalent

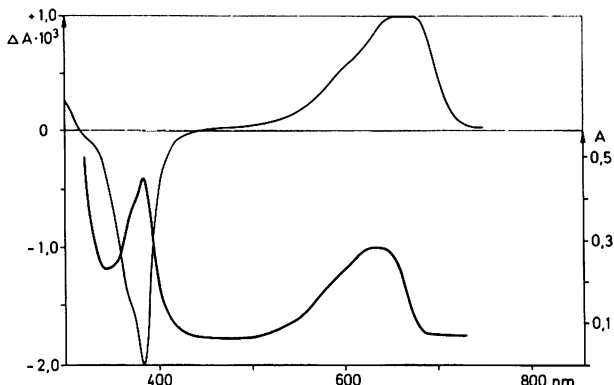


Fig. 5: Absorption (bottom) and CD-spectra (top) of a biliprotein from *Pieris brassica* (13). The pigment contains biliverdin $\text{IX}\gamma$ bound non-covalently to an apoprotein of MW $\approx 25\text{ kDa}$.

protein-chromophore interactions, which are reversible-lost upon unfolding of the protein, e.g. with urea (11). This type of interaction is probably characteristic for all phycobiliproteins and crucial to their function as antenna pigments, because they increase the oscillator strength of the visible band by almost one order of magnitude, and decrease the radiationless decay of excited states by more than three orders of magnitude (1). The specificity of these interactions can be seen by comparison with other biliproteins, e.g. the biliverdin $\text{IX}\alpha$ -serum albumin complex (12), or the biliverdin $\text{IX}\gamma$ -protein from *Pieris brassica* (13, see fig. 5). In both the latter pigments is the cyclic-helical conformation of the chromophores preserved, which is characteristic for the respective chromophores in solution (14,15). They have, accordingly, low fluorescence yields and weak absorptions in the visible range. Here, the major influence of the apoprotein is a preferential binding of one of the two helical enantiomers, which leads to intense induced CD-signals.

Due to the pronounced chromophore-protein interactions, the chromophores of PC can be used as very sensitive probes to monitor the state of the protein (1,11). Small aggregation-induced changes have been discussed in the first part. Much larger changes occur, if the protein is partially or fully unfolded, e.g. with urea or heat. After a previous study with PC from *S. platensis*, this method has now been used to investigate the stabilities of the PC and its subunits from *M. latus*.

The normalized absorption changes upon urea-denaturation are shown in fig. 6 (see legend for details). The gross changes are similar for the integral pigment (trimer) and its subunits. Small differences in the final (= 8M urea) absorptions are indicative of slightly different conformations of native chromophores, because the chromophores have the same molecular structure and are expected to have identical spectra in the denatured states. The most notable difference is the increased stability of the integral pigment, as compared to both subunits. At 4M urea, the absorption of the integral pigment is decreased by less than 4%, whereas the decrease of the subunits is 12% (α) and 15% (β). The urea concentrations necessary to induce a 50% decrease of the long-wavelength absorptions are 6.1, 5.6, 5.4M, respectively. In contrast to the results with PC from *S. platensis*, there are no indications for a stepwise unfolding evident from the absorption spectra.

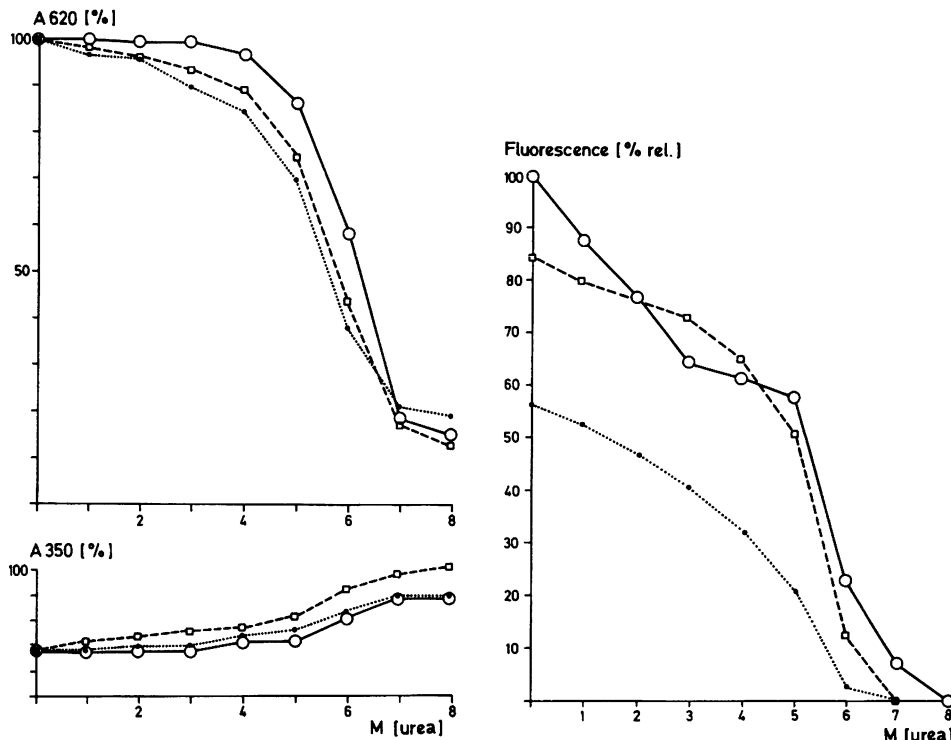


Fig. 6: Denaturation of trimeric PC (—) and its subunits (α :---; β :...) from M. laminosus with urea. Relative absorptions at the long-wavelength (top) and near-UV maxima (bottom), normalized to the absorptions in the absence of urea. All spectra were recorded from stock samples treated separately before the measurement with the appropriate amount of urea, either as 8M solution or as solid. All solutions in 100mM phosphate buffer, pH 7.5, $T = 25^\circ\text{C}$.

Fig. 7: Denaturation of PC from M. laminosus and its subunits with urea. Relative fluorescence intensities corrected for absorption. $\lambda_{\text{max}}, \text{exc.} = 600\text{nm}$; $\lambda_{\text{max}}, \text{em.} \approx 652\text{nm}$, decreasing with increasing urea concentration. Labels and details as in fig. 5.

The relative fluorescence yields during the same titration experiment are shown in fig. 7. There is already a large difference between the three species in their native states. The data for the integral pigment indicate a stepwise unfolding, with the first step being possibly related to the disaggregation of the trimer into monomers. The β -subunit is least stable (50% decrease at 3.5M urea), whereas α and the integral pigment have a 50% decrease at 5.3M urea. Although the curves of the last two species cross-over twice in the intermediate region, the sum of the subunits is always less than that of the integral pigment.

The differences of the thermal denaturation are even more pronounced among the three species (fig. 8). The "melting points" (50% decrease of the long-

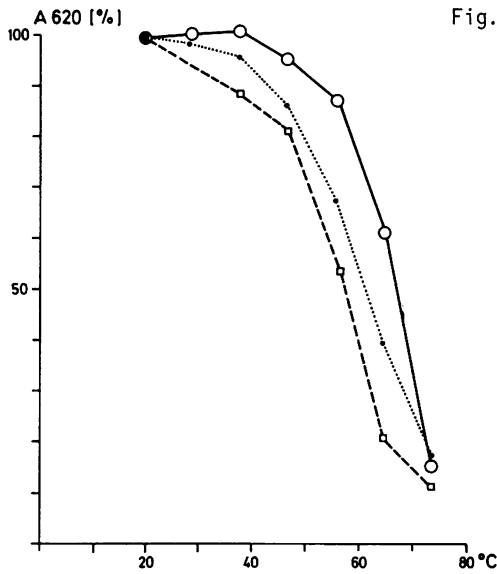


Fig. 8: Heat denaturation of PC. All spectra were recorded 5min after the sample had reached the temperature indicated. All measurements were done with fresh samples. Other details as in Fig. 5.

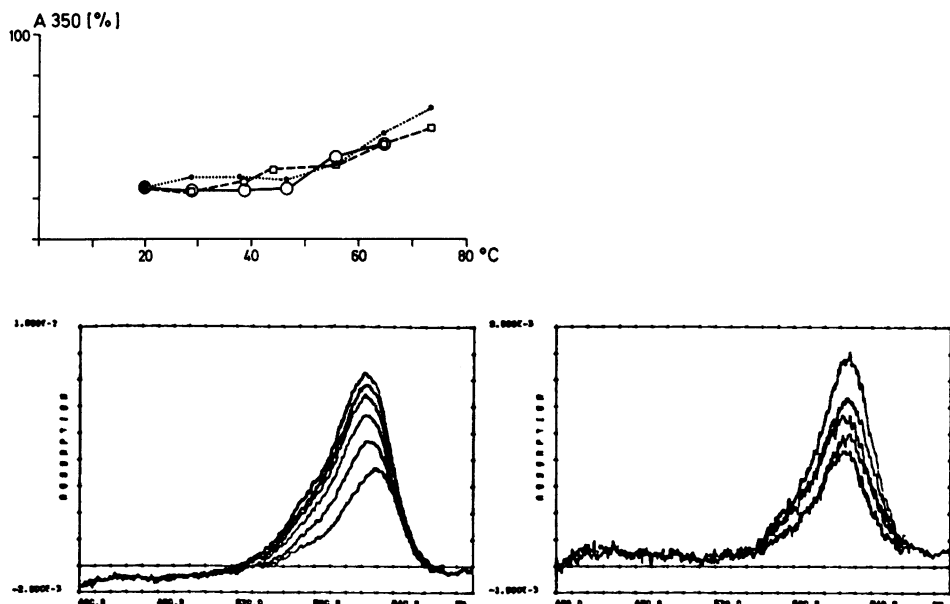


Fig. 9: Difference spectra for the photoreaction of PC in the presence of urea (5M). Top: Irradiation with 606nm light (interference filter). Positive bands correspond to bleaching. Bottom: Irradiation of the sample with 525nm light after saturating pre-irradiation at 606nm. Positive peaks correspond to increased absorptions.

wavelength absorption) is at 67° (PC), 61° (β) and 58° (α). The increase of thermal stability by almost 10° is significant with regard to the thermophilicity of *M. laminosus*, which grows well at temperatures as high as 55°C. At this temperature, the absorption of the integral pigment has decreased by only 10%. The "melting point" for PC from the mesophilic *S. platensis* is 52°C (11), i.e. 15°C below that of the thermophilic pigment.

The subunits differ also by their photochemical activities. PC is a light-harvesting pigment and its major deexcitation process in the isolated state is fluorescence. Another biliprotein, e.g. phytochrom, serves as "reaction center" pigment for photomorphogenesis in higher plants. Here, a structurally closely related chromophore is photochemically highly active. Several groups have reported recently that PC can undergo photochemical reactions, too, if it is partly denatured by a variety of reagents (see ref. 1 for leading references). This process is of potential significance also from a physiological point of view, because the reactions are similar to those of so-called phycocromes, which are thought to be sensory photoreceptors in blue-green alga. We have studied the photochemistry of PC and its subunits in the presence of increasing amounts of urea. The typical response of the sample is shown in fig. 7. Upon irradiation at 606nm, there is a bleaching of the long-wavelength maximum, which saturates rapidly. This bleaching is partially reversed upon irradiation at 525nm, but about the five-fold time is required for the back reaction.

In integral PC, this photochemical reaction is negligible in the absence of urea. It increases up to 4.5M of the denaturant, and then decreases again. The behavior can be rationalized by a model, in which the native chromophore is so tightly bound to the polypeptide chain, that it is unable to react photochemically. A partial denaturation of the polypeptide loosens these interactions sufficiently to allow for photochemical reactions, whereas a complete unfolding opens the channel for efficient radiationless deactivation and prohibits photochemistry as is typical for free biliverdins. The β -subunit shows a similar, but much more pronounced response, and the maximum reaction is again in the same region. The α -subunit is, by contrast, almost inactive and shows an irreversible bleaching at urea concentrations $\geq 5M$. This indicates again a rather specific environment of the different PC chromophores, with the photochemical activity being mostly located on the β -subunit.

The PC system is well suited for a detailed study of specific non-covalent chromophore protein interactions, which are crucial for the function of many chromoproteins. In combination with sensitive and selective spectroscopic methods, and the recent advances in structure analysis, a detailed picture of these interactions is expected in the near future.

Acknowledgements: This work was supported by the Deutsche Forschungsgemeinschaft.

References

1. H. Scheer: In F. K. Fong (ed.) "Light Reaction Path of Photosynthesis", p. 7 - 45, Springer-Verlag (1982)
2. A.N. Glazer: Ann. Rev. Biochem. 1983. 52, 125 (1983)
3. E. Gantt: Intern. Rev. Cytol. 66, 45 (1980)

4. P. Hefferle, W. John, H. Scheer, S. Schneider: Photochem. Photobiol. 39, 221 (1984)
5. W. Castenholz: Schweizer Z. Hydrol. 35, 538 (1970)
6. U.K. Laemmli: Nature 227, 680 (1970)
7. H. Lehner, H. Scheer: Z. Naturforsch. 38c, 353 (1983)
8. R. MacColl, K. Csatorday, D.S. Berns: Arch. Biochem. 208, 42 (1981)
9. T. Schirmer, W. Bode, R. Huber, W. Sidler, H. Zuber: J. Mol. Biol. 184, 257 (1985)
10. G. Frank, W. Sidler, H. Widmer, H. Zuber: Hoppe- Seyler s Z. Physiol. Chem. 359, 1491 (1978)
11. H. Scheer, W. Kufer: Z. Naturforsch. 32c, 513 (1977)
12. G. Wagniere, G. Blauer: J. Am. Chem. Soc. 98, 7806 (1976)
13. H. Kayser: Z. Naturforsch. 39c, 938 (1984)
14. H. Falk, G. Höllbacher: Monatsh. Chem. 109, 1429 (1978)
15. S.E. Braslavsky, A.R. Holzwarth, K. Schaffner: Angew. Chem. 95, 670 (1983), *ibid. Int. Ed.* 22, 656 (1983)